Dicle University
Journal of Engineering
https://dergipark.org.tr/tr/pub/dumf
duje.dicle.edu.tr

Research Article

A numerical and theoretical investigation into torsional buckling of composite driveshaft incorporating carbon nanotube

Hamza TAŞ[1*]

[1] Manisa Celal Bayar University, Mechanical Engineering Department, hamza.tas36@gmail.com, Orcid No: 0000-0002-6527-338X

ARTICLE INFO

Article history:

Received 2 August 2023
Received in revised form 11 December 2023
Accepted 12 December 2023
Available online 31 December 2023

Keywords:

Carbon nanotube, torsional buckling, micromechanical model, driveshaft, finite element analysis, laminated composite

Doi: 10.24012/dumf.1336638

* Corresponding author

ABSTRACT

Composite driveshafts have emerged as a potent substitute for traditional driveshafts because of their excellent strength-to-weight and stiffness-to-weight ratios. At the same time, usage of multi-walled carbon nanotubes (MWCNTs) as a reinforcement has gained a great momentum due to their superb mechanical, electrical, and thermal characteristics. In this work, a micromechanical model combining the rule of mixtures and the Halpin-Tsai (H-T) model was used to calculate elastic constants of MWCNTs-added carbon fiber reinforced epoxy resin. This micromechanical model considers the effect of agglomeration, aspect ratio, waviness, and random orientation of MWCNTs. Elastic constants of MWCNTs/epoxy resin calculated by using micromechanical model was compared by experimental results available in the literature. Moreover, finite element analysis (FEA) was carried out to predict the critical torsional buckling load of composite driveshafts for various MWCNTs concentrations and fiber orientation angles. The FEA results were compared with the results obtained theoretically. The results showed that Young's modulus of MWCNTs/epoxy resin calculated by using the micromechanical model follows the experimental findings. When compared to pure carbon fiber-reinforced epoxy resin, $\boldsymbol{E_1}$, $\boldsymbol{E_2}$, $\boldsymbol{G_{12}}$, and $\boldsymbol{G_{23}}$ (elastic constants of composite lamina) showed improvements of 0.66%, 27.80%, 49.02%, and 37.50%, respectively, in the case of 10vol.% MWCNTs addition. The ply orientation angle has a more dominant effect on $\boldsymbol{T_{cr}}$ than the MWCNTs concentration.

Introduction

Fiber-reinforced polymer (FRP) composites become more and more popular in automotive, aerospace, military, construction, and other industries due to their superior specific strength and stiffness compared to many traditional materials such as steel and aluminium [1]–[4]. Particularly in the automotive industry, composite materials have a wide range of applications. According to Ref. [5], by 2024, the automotive sector is predicted to be one of the top users of composite materials, with yearly consumption expected to exceed $15.5 billion.

The driveshaft one of the most critical parts of an automobile serves as the link between the engine and the axles and is responsible for transmitting the high torques that are applied to the wheels [6]–[10]. Conventional driveshafts commonly made of steel have a low cost of production and great fabricability but are massy. Since weight has a significant impact on automobile performance, it is practical to improve it by replacing traditional heavy drive shafts with composite ones. Weight savings ranging from 24% to 80% have been recorded by researchers [7], [11]–[13] when employing FRP composite driveshafts in place of steel driveshafts.

The design of a driveshaft is carried out based on the design specifications such as buckling torque capability, torque transmission capability, natural bending frequency, weight, and speed. A composite drive shaft was designed by Rangaswamy and Vijayarangan [14] using genetic algorithms for E-glass/epoxy and HM-carbon/epoxy composites with the goal of minimizing shaft weight while still meeting requirements for torsional buckling strength, torque transmission, and natural bending frequency. Kannan et al. [6] investigated the effect of stacking sequence and fiber orientation angles on the natural frequency, torsional stiffness, and buckling strength of a composite driveshaft. When compared to a typical steel shaft, composite materials led a significant weight reduction. The findings also showed that the torsional characteristics of the composite shafts are significantly influenced by the fiber orientation angle. Modelling and analysis of composite drive shafts for several ply angles and layer counts were performed and so the safest design criterion was determined by Altin et al. [7]. The numerical results showed that the 10-layer model with a winding angle of +/- 45 degrees has the lowest cost regarding strength. Gülşah [15] studied the torsional buckling behaviour of thin-walled rectangular cross-sectional composite tubes. Effects of tube length, cross section, and ply angle on the

critical torsional buckling load were investigated. The results revealed that critical torsional buckling load occurs between the ply angle of 20° and 40°. Critical buckling load increased with the decrease of tube length, but its impact is not as great as that of ply angle and edge rate. Rastogi [16] reported a study presenting a thorough method for designing driveshafts using automotive applications. Preliminary design tools meeting performance requirements such as critical speed, torsional strength, torsional buckling strength, and torsional fatigue for composite driveshafts were developed using closed-form analytical solutions and validated through in-depth finite element analyses. Shokrieh et al. [17] studied the torsional buckling behaviour of the composite driveshaft. Influences of ply angle, stacking sequence, and boundary conditions on the torsional buckling load were also examined. The findings demonstrated that the torsional buckling load is significantly influenced by fiber orientation and stacking sequence. They also concluded that finite element modelling enables a highly accurate prediction of the buckling torque.

The excellent electrical, mechanical, and thermal characteristics of carbon nanotubes (CNTs) have led to their recent consideration as potential nanoscale additives for polymer composites. Since CNTs have an elastic modulus and tensile strength in the range of 50-100 GPa and 1.4 TPa, respectively, introducing CNTs to polymers results in an increase of mechanical properties of polymers [18]. Schadler et al. [19] reported a 20% increase in tensile modulus and a 24% increase in compression modulus. Allaoui et al. [20] concluded that in comparison to pure resin matrix, the elasticity modulus and yield strength for composites containing 1 and 4 wt% carbon nanotubes, respectively, have increased by 2 and 4 times. Tai et al. [21] indicated 97.0% and 49.8% improvement in tensile strength and tensile modulus, respectively, when 3 wt% CNTs were added into the phenolic. Jain et al. [22] investigated the reinforcement effect of carbon fiber-epoxy(CF-EP) composites with CNTs and indicated that the ultimate tensile strength and interlaminar shear strength of CF-EP are increased by 17% and 28%, respectively, by the addition of 0.3 wt% CNTs.

To estimate the effects of CNT incorporation on the mechanical characteristics of the polymers, several micromechanical models have been suggested. In order to predict the elastic modulus of CNT-reinforced polymer nanocomposites Hassanzadeh-Aghdam et al. [23] constructed a micromechanical model that takes into account a number of significant parameters, such as the random orientation and distribution of wavy CNTs, the directional behaviour of CNTs, and the CNT/polymer interphase. Fisher et al. [24] created a model integrating finite element findings and micromechanical models to determine the effective modulus of wavy CNTs-reinforced polymer. Anumandla and Gibson [25] proposed a micromechanics model considering the curvature, length, and random arrangement of nanotubes for determining the effective elastic modulus of carbon nanotube-reinforced composites. Thostenson and Chao [26] revised the micromechanical model utilized for the modelling of short fiber composites to calculate the elastic modulus of the carbon nanotube-reinforced nanocomposite. The outcomes demonstrated that the elastic features of nanocomposites are significantly influenced by nanotube diameter. Seidel and Lagoudas [27] applied the Mori–Tanaka, self-consistent, and composite cylinders micromechanics approaches to calculate the Poisson's ratio, shear modulus, and elasticity modulus of aligned CNTs-reinforced nanocomposites. Pan et al. [28] created a model by exchanging effective fibers with wavy carbon nanotubes so as to investigate the effective elastic modulus of CNT/polymer composites, focusing on CNT waviness and agglomeration. The findings revealed that CNT-reinforced composites' elastic modulus is substantially influenced by agglomeration and waviness.

The main objective of this study is to examine the effects of MWCNT on the critical torsional buckling load of composite driveshafts numerically and theoretically. In this study, elastic constants of MWCNTs-added carbon fiber-reinforced epoxy resin were calculated using a micromechanical model that combines the rule of mixtures and the Halpin-Tsai (H-T) model. The impact of MWCNT aggregation, aspect ratio, waviness, and random orientation is considered by this micromechanical model. Elastic constants of MWCNTs/epoxy resin computed by using a micromechanical model were compared with the published experimental results. The critical torsional buckling load of composite driveshafts is also predicted using finite element analysis (FEA) for different MWCNT concentrations and fiber orientation angles. The results of the FEA were compared to those found theoretically. Additionally, a regression equation was constructed that gives the variation of the critical torsional buckling load of composite driveshaft with the change of ply orientation angle and MWCNT concentration.

Micromechanical model

Elastic constants of CNTs-reinforced polymer matrix

Understanding the mechanical behaviour of CNT-reinforced polymer composites under torsional loads requires knowledge of elastic constants such as elasticity modulus, Poisson's ratio, and shear modulus. In this work, the mechanical properties of CNTs-based polymer composites were determined by combining the rule of mixtures and the Halpin-Tsai (H-T) model. This combined model considers the impacts of agglomeration, random orientation, aspect ratio, and waviness of CNTs in the matrix when calculating the mechanical properties of nanocomposite [29]–[31].

The elasticity modulus of the straight-aligned CNTs incorporated polymers (E_{m-CNT}) can be predicted by using the following H-T model [29]:

$$E_{C/M} = \left(E_{CNT/m} - 1\right)V_{CNT} \qquad (1)$$

where $E_{C/M}$ and $E_{CNT/m}$ can be calculated by utilizing Equation (2) and (3).

$$E_{C/M} = \frac{E_{m-CNT} - E_m}{E_m} \quad (2)$$

$$E_{CNT/m} = \frac{E_{CNT}}{E_m} \quad (3)$$

In Equations (1), (2), and (3), E_m, E_{CNT}, and E_{m-CNT} are Young's modulus of polymer matrix, carbon nanotube, and carbon nanotube incorporated polymer matrix, respectively. V_{CNT} denotes the volume fraction of carbon nanotubes in the polymer matrix. $E_{CNT/m}$ is the ratio of the Young's modulus of the carbon nanotube to that of the polymer matrix. As already mentioned, Equation (1) can only be used to calculate straight-aligned CNTs reinforced polymers. However, in real-world situations, agglomeration, random orientation, and waviness of the CNTs embedded in the matrix have a significant impact on the mechanical properties. Besides, aspect ratio of CNTs plays an important role in the mechanical characteristics of CNTs-reinforced polymers. Therefore, adding random orientation factor β_R, waviness factor β_W, and length efficiency factor β_L to Equation (1) enables to predict the elasticity modulus of CNT-reinforced polymers with sufficient accuracy. As a result, Equation (1) can be rewritten as

$$E_{C/M} = \left(\beta_R \beta_W \beta_L E_{CNT/m} - 1\right) V_{CNT} \quad (4)$$

where random orientation factor β_R is 1/3 and 1/5 for 2-D (in-plane) and 3-D situations, respectively. Length efficiency factor β_L takes a value in the range of 0 and 1 and can be determined by using Equation (5):

$$\beta_L = \frac{tanh\lambda\tau}{\lambda\tau} \quad (5)$$

in which λ is the aspect ratio of CNT. λ and τ parameters can be determined as follows:

$$\lambda = \frac{2l}{d} \quad (6)$$

$$\tau = \sqrt{\frac{-2}{E_{CNT/m}(1-\upsilon_m) ln\,(V_{CNT})}} \quad (7)$$

where d and l are the diameter and length of the CNT, respectively. υ_m states the Poisson's ratio of the matrix. Both CNT aspect ratio and volume fraction of CNT in the matrix are crucial for the length efficiency factor. Therefore, β_L approaches one for high aspect ratios and large volume fractions. The waviness factor β_W is equal to one for the straight CNTs, but less than one for wavy CNTs. β_W can be determined by

$$\beta_W = 1 - \frac{a}{w} \quad (8)$$

where w and a represent the half-wavelength and amplitude of the curving CNT.

Even though the relationship between the E_{m-CNT} and V_{CNT} is linear according to Equation (4), many experimental research [32]–[36] concluded a non-linear relationship between the E_{m-CNT} and V_{CNT}. This non-linear relationship is due to the increasing tendency of carbon nanotubes to agglomerate as the CNTs fraction in the matrix rises. Thus, Equation (4) is modified by the addition of the agglomeration factor β_A.

$$E_{C/M} = \left(\beta_R \beta_W \beta_L E_{CNT/m} - 1\right) V_{CNT} \beta_A \quad (9)$$

In Equation (9), β_A can be determined by

$$\beta_A = exp\left(-\alpha V_{CNT}^{\beta}\right) \quad (10)$$

where α and β parameters are associated with the agglomeration degree of CNTs in the matrix. α and β parameters are considered as 9 and 0.9, respectively [30].

Given that the CNTs-reinforced polymer matrix behaves in a quasi-isotropic manner, the following equation can be used to determine its shear modulus [4]:

$$G_{m-CNT} = \frac{E_{m-CNT}}{2(\upsilon_{m-CNT} + 1)} \quad (11)$$

where Poisson's ratio of CNTs-based polymer matrix (υ_{m-CNT}) is equal to Poisson's ratio of polymer matrix (υ_m).

The equation as follows can be used to compute the density of the CNTs-based polymer matrix:

$$\rho_{m-CNT} = \rho_{CNT} V_{CNT} + \rho_m V_m \quad (12)$$

where ρ_m and ρ_{CNT} are respectively the densities of polymer matrix and carbon nanotube. V_m symbolizes the volume fraction of the polymer matrix in the CNTs-added polymer matrix.

Elastic constants of unidirectional lamina

The elasticity modulus of a unidirectional lamina longitudinal direction, E_1, density, ρ_c, and Poisson's ratio, υ_{12}, can be computed by using the mixture rule [37].

$$E_1 = E_f V_f + E_{m-CNT} V_{m-CNT} \quad (13)$$

$$\rho_c = \rho_f V_f + \rho_{m-CNT} V_{m-CNT} \quad (14)$$

$$\upsilon_{12} = \upsilon_f V_f + \upsilon_{m-CNT} V_{m-CNT} \quad (15)$$

where E_f, ρ_f, and υ_f denote Young's modulus, density, and Poisson's ratio of fiber, respectively. V_f is fiber volume fraction in the lamina. In the present study, V_f and V_{m-CNT} were taken to be 60% and 40%, respectively. Since using the rule of mixture to calculate the elasticity modulus in the transverse direction, E_2, Poisson's ratio, υ_{12}, and shear modulus', G_{12} and G_{23} don't give sufficiently consistent

results with experimental data, the modified H-T equation can be utilized to compute these elastic constants [38].

$$\frac{P}{P_{m-CNT}} = \frac{1+\xi\eta V_f}{1-\eta V_f} \quad (16)$$

where P_{m-CNT} is the corresponding properties of the CNTs-based polymer matrix. P can be regarded as E_2, υ_{12}, G_{12} and G_{23}. η is an experimental parameter and can be computed by using the following equation.

$$\eta = \frac{\frac{P_f}{P_{m-CNT}} - 1}{\frac{P_f}{P_{m-CNT}} + \xi} \quad (17)$$

where P_f and P_{m-CNT} mean corresponding properties of fiber and CNTs-based polymer matrix. Reinforcing factor ξ can be chosen as 2 for E_2 calculation and 1 for υ_{23}, G_{12}, and G_{23} calculation [37].

Critical torsional buckling load of composite driveshafts

Since composite driveshafts are designed as long, thin and hollow structures, they are susceptible to torsional buckling under a torsion load. Critical torsional buckling load, T_{cr}, for thin-walled orthotropic driveshafts can be determined by [14]

$$T_{cr} = (2\pi r^2 t)(0.272)\left(E_x E_y^3\right)^{1/4}\left(\frac{t}{r}\right)^{3/2} \quad (18)$$

where E_x and E_y are the elasticity modulus of composite driveshaft in the direction of axial and hoop, respectively. t and r state the thickness and mean radius of the composite driveshaft. Equation (18), which is commonly used to design driveshafts, was developed from the equation for an isotropic cylindrical shell.

Finite element analysis

The finite element method (FEM), a numerical method, is used to find the approximate solution of partial differential equations. FEM can be used to solve problems in a variety of engineering and mathematical physics fields, such as heat transfer, mass transport, structural analysis, fluid flow, and electromagnetic potential. FEM breaks down a complex system into smaller pieces known as finite elements to solve a problem. FEM generates equations for each finite element and then merges them to get the solution for the entire structure rather than solving the problem for the whole structure in just one step [39].

In this study, a commercially available finite element analysis (FEA) program, ANSYS 22 R2 was used to find the critical torsional buckling loads of composite driveshafts subjected to the torsion load. ANSYS Composite PrepPost (ACP), an integrated tool in the Ansys Workbench environment, was used to model the composite driveshaft. ACP uses the Ansys Mechanical solvers to carry out structural, thermal, and fluid-solid interaction simulations. ACP enables to create laminated composites defined layer-by-layer [40].

In this study, LY 5052 Epoxy resin, AS4 Carbon fiber, and multi-walled carbon nanotubes (MWCNTs) were used as matrix material, reinforcing material, and nanofiller. Some material properties of these components are illustrated in Table 1.

Table 1. Mechanical properties of nanocomposite components

LY5052 Epoxy resin [30]		AS4 Carbon fiber [41]		MWCNTs [30]	
E_m(GPa)	3.11	E_{f11}(GPa)	225	E_{CNT}(GPa)	900
G_m(GPa)	1.152	E_{f22}(GPa)	15	L_{CNT}(nm)	2000
υ_m	0.35	G_{f12}(GPa)	15	d_{CNT}(nm)	3
ρ_m(g/cm^3)	1.17	G_{f23}(GPa)	7	ρ_{CNT}(g/cm^3)	2.25
		υ_{f12}	0.20		
		υ_{f23}	0.40		
		ρ_f(g/cm^3)	1.79		

The elastic constants of MWCNTs-reinforced LY5052 epoxy resin for the MWCNTs volume fractions of 0.0, 0.25, 0.5, 1.0, 1.5, 2.0, 3.0, 4.0, 6.0, 8.0 and 10%.was determined by Equations (1)-(11). Then, elastic constants of MWCNTs-incorporated AS4 carbon fiber/LY5052 epoxy resin were obtained by using Equations (13-(17). These elastic constants were used in the FEA.

In the current work, a composite driveshaft with inner and outer diameters of 40 and 44 mm and made of eight laminas with a uniform thickness of 0.25 mm was modelled. The length of the composite driveshaft is 500 mm. A schematic view of the composite driveshaft and its dimensions are illustrated in Fig. 1.

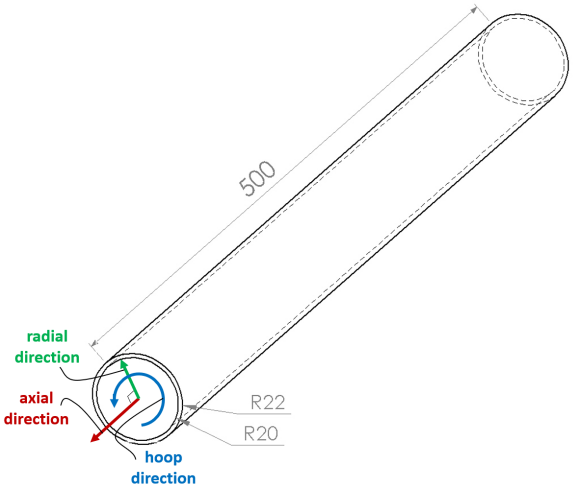

Figure 1. Schematic view of composite driveshaft (Dimensions are in mm)

A two-dimensional surface mesh with 16002 Quad4 elements and 16065 nodes was generated to carry out the torsional buckling analysis. The resulting surface mesh is displayed in Fig. 2.

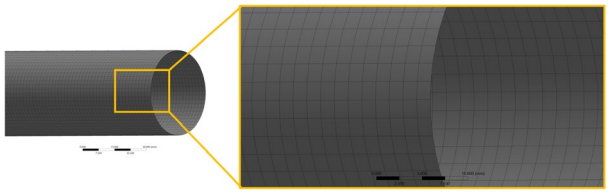

Figure 2. Mesh configuration

In FEA, the composite driveshaft was exposed to torsional load of 1 Nm at one end while being fixed in all directions at the other. Following the static analysis of the composite driveshaft, stress results are recorded to compute the torsional buckling load. Torsional buckling load is calculated by multiplying static torsional load and load multiplier.

Results and discussion

Effects of MWCNTs inclusion on the mechanical properties of epoxy resin

The mechanical properties of MWCNTs-reinforced epoxy resin which were theoretically calculated for various volume fractions are presented in Table 2. The inclusion of MWCNTs into the epoxy resin causes a remarkable increase in elasticity modulus, shear modulus, and density. Approximately 17%, 52%, and 72% improvements occur in Young's modulus and shear modulus in the case of 1.0vol.%, 4.0vol.%, and 10.0vol.% MWCNTs addition. However, density increases only 0.8%, 3.2%, and 8.0% when 1.0vol.%, 4.0vol%, and 10.0vol.% MWCNTs are added. This means 16%, 47%, and 59% increments in specific elastic and shear moduli for additions of 1.0vol.%, 4.0vol.%, and 10.0vol.% MWCNTs, respectively. Increments in specific elastic and shear moduli are smaller than the increases in elastic and shear moduli due to the non-linear relationship between the elastic/shear modulus and MWCNTs volume fraction, but the linear relationship between the density and MWCNTs volume fraction.

Table 2. Mechanical properties MWCNTs-included epoxy resin

V_{CNT} (vol%)	E_{m-CNT} (GPa)	G_{m-CNT} (GPa)	ρ_{m-CNT}(g/cm^3)
0.00	3.110	1.152	1.250
0.25	3.251	1.204	1.253
0.50	3.390	1.255	1.255
1.00	3.649	1.351	1.260
1.50	3.883	1.438	1.265
2.00	4.092	1.516	1.270
3.00	4.445	1.646	1.280
4.00	4.721	1.749	1.290
6.00	5.091	1.886	1.310
8.00	5.280	1.956	1.330
10.00	5.344	1.979	1.350

Fig. 3 shows how the elastic modulus of epoxy resin reinforced with MWCNTs changes as a function of the MWCNTs concentration. In Fig. 3, It is clear that as the MWCNTs volume fraction increases, Young's modulus increases, but at a decreasing rate due to the agglomeration of MWCNTs. Duan et. al [34] also reported a decrease in Young's modulus for the MWCNTs concentration greater than 0.6 wt%. Fig. 3 demonstrates a high degree of consistency between the findings of the current study and those of Omidi et al. [29]. It is obvious that adding factors such as random orientation, waviness, length efficiency, and agglomeration into the H-T model resulted in a good agreement between predictions and experimental findings.

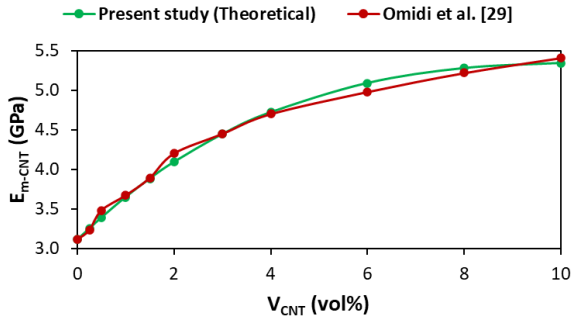

Figure 3. Variation of elasticity modulus of MWCNTs-based epoxy resin with MWCNTs volume fraction ($\beta_r = 0.2$, $\lambda = \frac{2l}{d}$ where $l = 2000nm$ and $d = 30nm$, $\upsilon_m = 0.35$, $\beta_w = 0.5$, and $\beta_A = exp(-\alpha V_{CNT}^{\beta})$ where $\alpha = 9$ and $\beta = 0.9$)

The effect of the MWCNT waviness on the elastic modulus of MWCNTs-based epoxy resin as a function of MWCNTs concentration is presented in Fig. 4. It is obvious that the waviness of MWCNTs plays a critical role in elastic modulus. As the waviness factor increases, which means straighter MWCNT, Young's modulus rises. With increasing MWCNT concentrations, this rise becomes more pronounced. Paunikar and Kumar [42] also reported a considerable decrease in effective Young's modulus even with small waviness. Additionally, predicted results calculated for the waviness factor of 0.5 are in good agreement with the experimental results obtained by Omidi et al. [29].

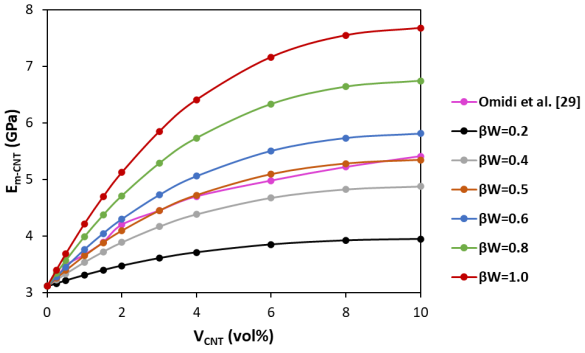

Figure 4. Variation of elasticity modulus of MWCNTs-based epoxy resin with MWCNTs volume fraction depending on the β_w waviness factor fraction ($\beta_r = 0.2$, $\lambda = \frac{2l}{d}$ where $l = 2000m$ and $d = 30nm$, $\upsilon_m = 0.35$, and $\beta_A = exp(-\alpha V_{CNT}^{\beta})$ where $\alpha = 9$ and $\beta = 0.9$)

Influence of the MWCNT length on Young's modulus of MWCNTs-reinforced epoxy resin as a function of MWCNTs volume fraction is illustrated in Fig. 5. As it can be seen from Fig. 5, the length of the MWCNT has a significant impact on Young's modulus of MWCNTs-

reinforced epoxy resin. As the length of the MWCNT rises, the elastic modulus of epoxy resin reinforced with MWCNTs increases. This increase is more pronounced for MWCNTs shorter in length. After a certain length of the MWCNT (approximately 4 μm), further increasing the length of the MWCNT has a negligible effect on the elastic modulus (Fig. 6). A similar trend has also been observed by Aghadavoudi et al. [43].

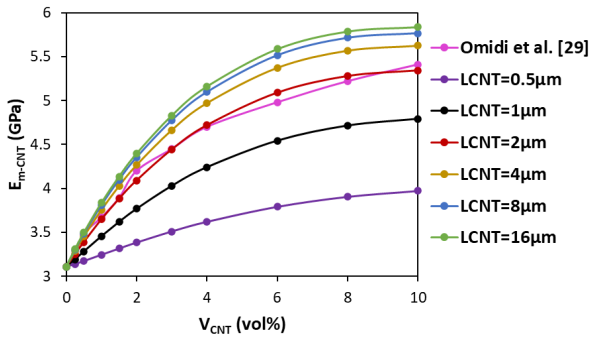

Figure 5. Variation of elasticity modulus of MWCNTs-based epoxy resin with MWCNTs volume fraction depending on the aspect ratio of MWCNTs ($\beta_r = 0.2$, $\lambda = \frac{2l}{d}$ where $d = 30nm$, $\upsilon_m = 0.35$, $\beta_w = 0.5$, and $\beta_A = exp\left(-\alpha V_{CNT}^{\beta}\right)$ where $\alpha = 9$ and $\beta = 0.9$)

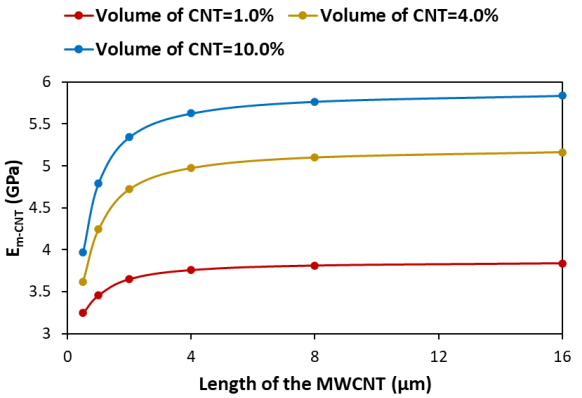

Figure 6. Variation of elasticity modulus of MWCNTs-reinforced epoxy resin with the length of the MWCNT

Elastic constants of MWCNTs-added carbon fiber-reinforced epoxy resin

The elastic constants of the unidirectional composite lamina for various MWCNTs volume fractions are presented in Table 3. These elastic constants were used as input data for FEA. It is obvious that while MWCNT concentration has a negligible effect on E_1, it has a considerable impact on E_2, G_{12}, and G_{23}. Elasticity modulus in the longitudinal direction for unidirectional laminates is dominantly controlled by the continuous fibers rather than MWCNTs. Therefore, the rise in E_1 is negligible when compared to the increase in E_2, G_{12}, and G_{23} [44]. Compared to pure carbon fiber-reinforced epoxy resin, there is a 0.66%, 27.80%, 49.02%, and 37.50% improvement in E_1, E_2, G_{12}, and G_{23} in the case of 10vol.% MWCNTs inclusion (Fig. 7). Increase in elastic constants declines as the MWCNTs concentration rises because of non-homogeneous dispersion of MWCNTs.

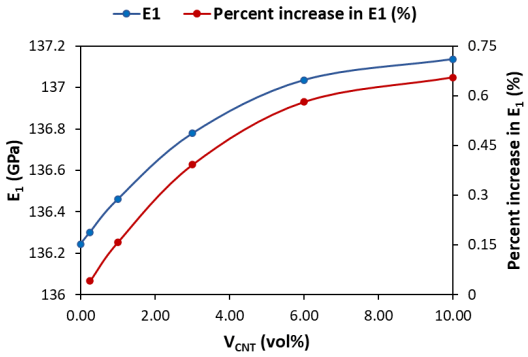

(a)

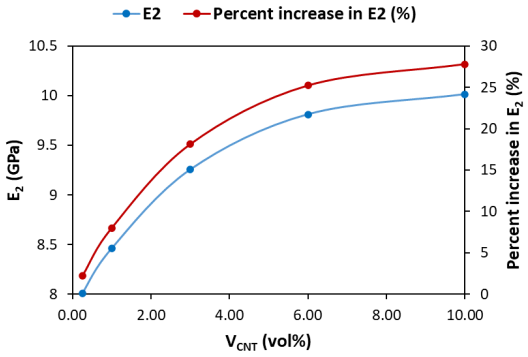

(b)

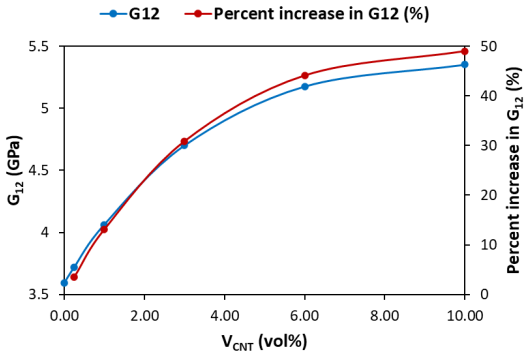

(c)

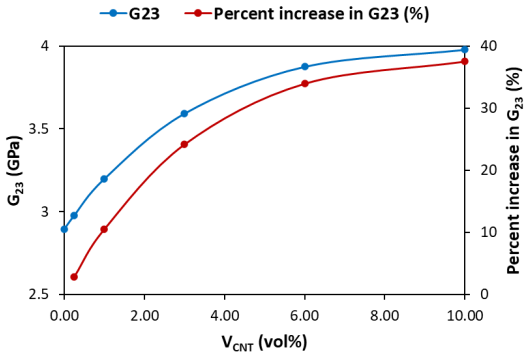

(d)

Figure 7. Variation of (a) E_1, (b) E_2, (c) G_{12}, and (d)G_{23} of unidirectional composite lamina with the MWCNTs volume fraction

Table 3. Variation of elastic constants of the unidirectional composite lamina with MWCNTs concentration

V_{CNT} (vol%)	0.00	0.25	1.00	3.00	6.00	10.00
E_1 (GPa)	136.244	136.300	136.460	136.778	137.036	137.137
E_2 (GPa)	7.835	8.008	8.462	9.255	9.811	10.013
G_{12} (GPa)	3.592	3.719	4.063	4.701	5.177	5.353
G_{23} (GPa)	2.893	2.976	3.197	3.592	3.875	3.978
υ_{12}	0.260	0.260	0.260	0.260	0.260	0.260
υ_{23}	0.379	0.379	0.379	0.379	0.379	0.379

Effect of MWCNTs inclusion on the critical torsional buckling load of composite driveshaft

The critical torsional buckling load of the composite driveshaft was predicted both numerically and theoretically. Critical torsional buckling load computed by using Equation (18) for various MWCNTs concentrations was compared with those from FEA. The variation of the critical torsional buckling load of composite driveshaft with the change of MWCNTs volume fraction and percentage error (%) between the FEA and theoretical results are presented in Fig. 8. It is clear from Fig. 8 that as the MWCNTs content increases critical torsional buckling load rises. However, after a certain MWCNTs content (6.0vol.%), the effect of MWCNTs on the critical torsional buckling load is negligible. For theoretical and numerical calculations, the 10.0vol.% MWCNT addition to pure lamina results in increases of 20.4% and 26.7%, respectively. For all MWCNT concentrations, the critical torsional buckling load predicted numerically is higher than those calculated theoretically. The highest percentage error is 5.1%, indicating that the theoretical and numerical results are in good agreement. Therefore, the following investigations were carried out by using FEA.

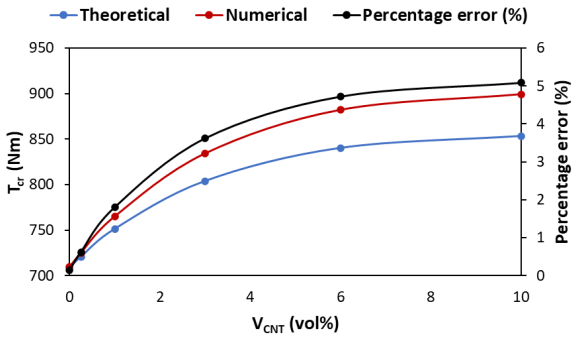

Figure 8. Variation of critical torsional buckling load of $[0]_8$ composite driveshaft for various MWCNTs concentrations

In this study, the effect of ply orientation angle on the critical torsional buckling load was examined by using FEA. Fig. 9 illustrates the change of critical buckling load for various ply orientation angles. As it can be seen from Fig. 9, the ply orientation angle has a significant influence on the critical torsional buckling load. When compared to 0° ply orientation angle, critical torsional buckling load reduces by 8.7% and 3.9% for 30° and 45° ply orientation angles, respectively. However, further increasing the ply orientation angle results in a sharp increase in critical buckling load. Critical torsional buckling load increases by 30.9% and 201.9% for 60° and 90° ply orientation angles, respectively, in comparison to 0° ply orientation angle. Badie et al. [45] also reported that 90° ply orientation angle is the best for the peak torsional buckling. The fibers aligned in the hoop direction at this ply orientation angle result in an increasing modulus (E_y). Since T_{cr} is directly proportional to the cube of E_y according to Equation (18), T_{cr} increases as the ply orientation angle increases. The highest value of the buckling torque is reached when the fibers are orientated at 90 degrees since the expression of buckling torque is dominantly related to the elasticity modulus of the composite driveshaft in the hoop direction.

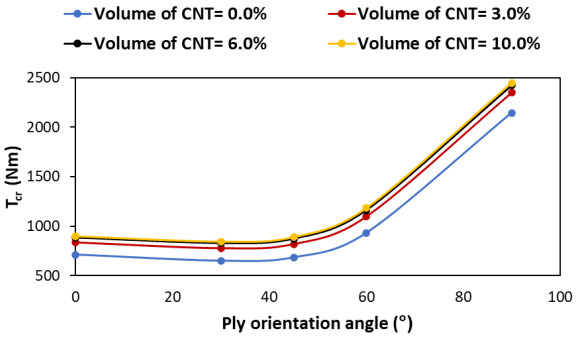

Figure 9. Variation of critical torsional buckling load of composite driveshaft with the change of ply orientation angle

3D surface and contour plots showing the variation of critical torsional buckling load with MWNCTs content and ply orientation angle are illustrated in Fig. 10. According to Fig. 10, the ply orientation angle of continuous carbon fibers dominates the critical torsional buckling load rather than MWCNTs. Furthermore, it is evident that the ply orientation angle has no bearing on the beneficial effects of MWCNTs on T_{cr}, excluding the 90° ply orientation angle. Increases in T_{cr} are 26.7%, 30.4%, 30.7%, 27.3%, and 14.2% in the case of 10vol.% MWCNTs addition compared to pure lamina for 0°, 30°, 45°, 60°, and 90° ply orientation angle, respectively. At a 90° ply orientation angle, the beneficial effect of MWCNTs on T_{cr} decreases.

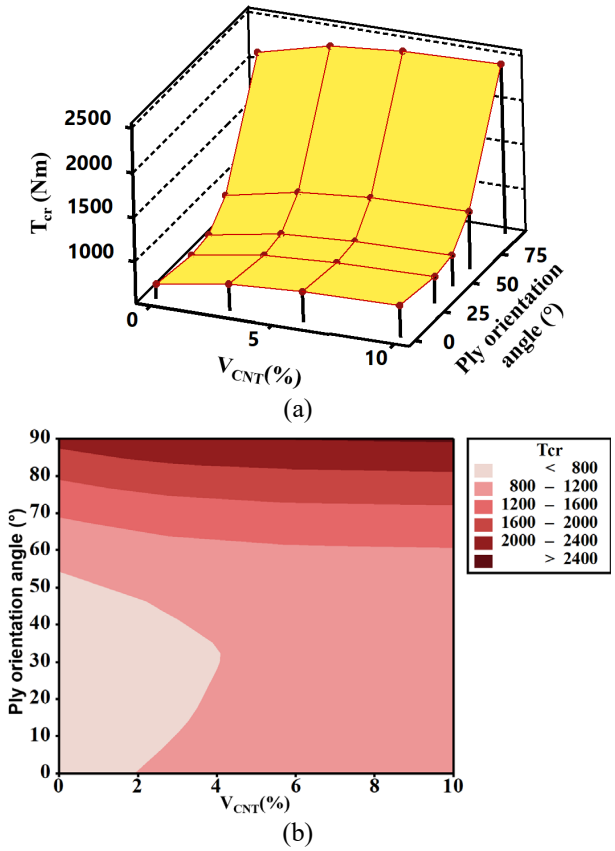

Figure 10. a) 3D surface and b) Contour plot of critical torsional buckling load versus MWCNTs concentration and ply orientation angle

Table 4. Comparison of T_{cr} values obtained by FEA and by using regression equation

V_{CNT} (vol.%)	θ (°)	T_{cr} (Nm)-FEA	T_{cr} (Nm)-Reg.Eq	Relative error (%)
0	0	709.87	676.73	-4.67
0	30	648.06	752.88	16.17
0	45	682.18	671.17	-1.61
0	60	929.54	849.39	-8.62
0	90	2143.90	2145.45	0.07
3	0	834.11	804.63	-3.53
3	30	776.03	876.87	12.10
3	45	817.83	804.84	-1.59
3	60	1095.40	1037.80	-5.26
3	90	2347.50	2397.97	2.15
6	0	881.96	839.95	-4.76
6	30	826.75	906.56	9.65
6	45	871.83	835.41	-4.18
6	60	1160.00	1083.89	-6.56
6	90	2421.40	2451.30	1.23
10	0	899.11	887.39	-1.30
10	30	845.11	941.27	11.38
10	45	891.41	864.99	-2.96
10	60	1183.20	1113.13	-5.92
10	90	2447.40	2470.98	0.96

In order to have a better comprehension of the relationship between the critical torsional buckling load, fiber orientation angle, and MWCNTs concentration, a regression equation with the $R^2 = 99.07$ was constructed as follows:

$$T_{cr} = 743.00 + 50.20V_{CNT} - 17.76\theta - 3.34V_{CNT}^2 + 0.37\theta^2 + 0.126V_{CNT}\theta \quad (19)$$

where θ denotes the ply orientation angle. Table 4 shows the T_{cr} values obtained by FEA and by using Equation (19). It is obvious that this regression equation can accurately predict the T_{cr} value with an average error of 5.28%.

Fig. 11a, b, c, and d illustrate the effect of MWCNTs volume fraction on the first mode shape of torsional buckling whereas Fig. 11b, e, f, g, and h show the influence of ply orientation angle on the first mode shape of torsional buckling. As shown in Fig. 11, MWCNT concentration has no impact on the first mode shape, but the ply orientation angle significantly alters it. As the ply orientation angle rises, number of circumferential waves increases. Moreover, it is obvious that all composite driveshafts exhibit helical buckling mod.

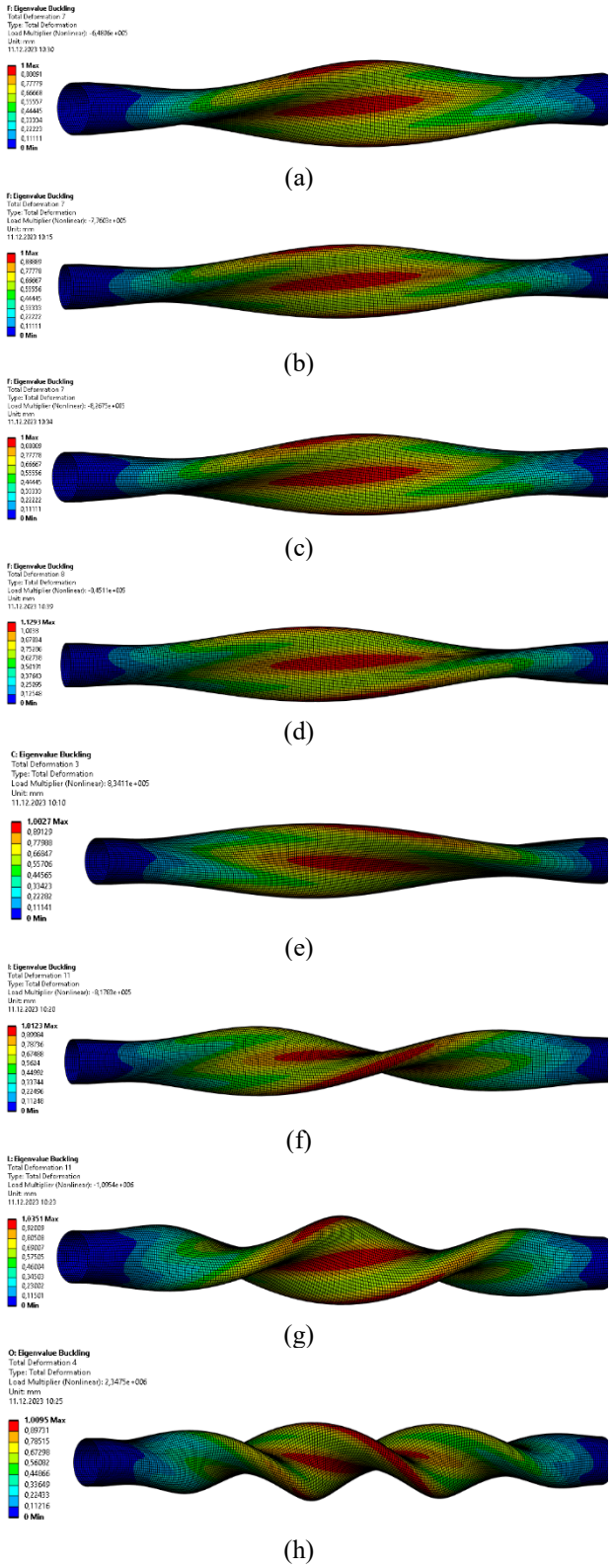

Figure 11. First mode shape of torsional buckling for the composite driveshaft with a) $V_{CNT} = 0.0vol.\%$ and $\theta = 30°$ b) $V_{CNT} = 3.0vol.\%$ and $\theta = 30°$ c) $V_{CNT} = 6.0vol.\%$ and $\theta = 30°$ d) $V_{CNT} = 10.0vol.\%$ and $\theta = 30°$ e) $V_{CNT} = 3.0vol.\%$ and $\theta = 0°$ f) $V_{CNT} = 3.0vol.\%$ and $\theta = 45°$ g) $V_{CNT} = 3.0vol.\%$ and $\theta = 60°$ h) $V_{CNT} = 3.0vol.\%$ and $\theta = 90°$

Conclusions

The following conclusions can be made:

- Introducing MWCNTs into the epoxy resin results in a notable improvement in elasticity modulus, shear modulus, and density. When 1.00%, 4.00%, and 10% MWCNTs are included into epoxy resin, Young's modulus and shear modulus, respectively, improve by around 17%, 52%, and 72%.
- The waviness and length of the MWCNT have a great influence on Young's modulus of MWCNTs/epoxy resin. Increase of both waviness factor which means straighter MWCNT and length results in a boost of elastic modulus.
- While MWCNTs concentration has an insignificant impact on the E_1, it considerably affects the E_2, G_{12}, and G_{23}.
- The addition of 10vol.% MWCNT to pure lamina raises T_{cr} by 20.4% and 26.7%, respectively, according to the theoretical and numerical calculations.
- Critical torsional buckling load decreases by 8.7% and 3.9% for 30° and 45° ply orientation angles, respectively, when compared to 0° ply orientation angle. But as the ply orientation angle is increased further, the critical buckling load increases dramatically. For 60° and 90° ply orientation angles, respectively, the critical torsional buckling load rises by 30.9% and 201.9% as compared to the 0° ply orientation angle.
- Except for the 90° ply orientation angle, the ply orientation angle has little to no impact on the favorable effects of MWCNTs on T_{cr}.
- All composite driveshafts buckle in a helical mode.

Ethics committee approval and conflict of interest statement

There is no need to obtain permission from the ethics committee for the article prepared.

There is no conflict of interest with any person / institution in the article prepared.

Author Contribution

Every section of the paper is prepared by Hamza TAŞ.

References

[1] H. Taş and I. F. Soykok, "Effects of carbon nanotube inclusion into the carbon fiber reinforced laminated composites on flexural stiffness: A numerical and theoretical study," *Compos. Part B Eng.*, vol. 159, pp. 44–52, Feb. 2019, doi: 10.1016/j.compositesb.2018.09.055.

[2] E. M. Soliman, M. P. Sheyka, and M. R. Taha, "Low-velocity impact of thin woven carbon fabric composites incorporating multi-walled carbon nanotubes," *Int. J. Impact Eng.*, vol. 47, pp. 39–47, Sep. 2012, doi: 10.1016/j.ijimpeng.2012.03.002.

[3] J. Galos, "Thin-ply composite laminates: a review," *Compos. Struct.*, vol. 236, p. 111920, Mar. 2020, doi: 10.1016/j.compstruct.2020.111920.
[4] S. K. Georgantzinos, P. A. Antoniou, G. I. Giannopoulos, A. Fatsis, and S. I. Markolefas, "Design of Laminated Composite Plates with Carbon Nanotube Inclusions against Buckling: Waviness and Agglomeration Effects," *Nanomaterials*, vol. 11, no. 9, Art. no. 9, Sep. 2021, doi: 10.3390/nano11092261.
[5] "Automotive Composites Market Size, Share & Global Forecast Analysis: 2019-2024," Stratview Research, SRTI130, Oct. 2019. Accessed: Jul. 18, 2023. [Online]. Available: https://www.stratviewresearch.com/581/automotive-composites-market.html
[6] R. Kannan, I. D. Lawrence, G. Kaviprakash, and A. Regan, "Design and Analysis of Composite Drive Shaft for Automotive Application," *Int. J. Eng. Res. Technol.*, vol. 3, pp. 429–436, Aug. 2014.
[7] B. Altin, A. A. Bekem, and A. Ünal, "Determination of Design Criteria for Composite Drive Shaft in Automobiles," *Politek. Derg.*, pp. 1–1, Dec. 2023, doi: 10.2339/politeknik.1028437.
[8] S. K. S. Nadeem, G. Giridhara, and H. K. Rangavittal, "A Review on the design and analysis of composite drive shaft," *Mater. Today Proc.*, vol. 5, no. 1, Part 3, pp. 2738–2741, Jan. 2018, doi: 10.1016/j.matpr.2018.01.058.
[9] A. Bolshikh, "Computational and experimental study of the strength of a composite drive shaft," *Transp. Probl.*, vol. 16, no. 1, p. 75, 2021.
[10] V. Chougule, A. Gupta, and S. Chavan, "Design and Manufacturing of Carbon Fiber Composite Drive Shaft as an Alternative to Conventional Steel Drive Shaft," *Int. J. Innov. Sci. Res. Technol.*, vol. 3, no. 10, pp. 674–683, 2018.
[11] A. Ravi, "Design, Comparison and Analysis of a Composite Drive Shaft for an Automobile," *Int. Rev. Appl. Eng. Res.*, vol. 4, no. 1, pp. 21–28, 2014.
[12] V. S. Bhajantri, S. C. Bajantri, A. M. Shindolkar, and S. S. Amarapure, "DESIGN AND ANALYSIS OF COMPOSITE DRIVE SHAFT," *Int. J. Res. Eng. Technol.*, vol. 3, no. 3, pp. 738–745, 2014.
[13] B. Gireesh, S. Shrishail B, and V. N. Satwik, "Finite Element & Experimental Investigation of Composite Torsion Shaft," *Int. J. Eng. Res. Appl.*, vol. 3, no. 2, pp. 1510–1517, 2013.
[14] T. Rangaswamy and S. Vijayarangan, "Optimal Sizing and Stacking Sequence of Composite Drive Shafts," vol. 11, Jan. 2005.
[15] G. ALAR ÖNER, "Torsional Buckling to Thin Walled Composite Tubes," Ph.D. Thesis, Atatürk University, 2009.
[16] N. Rastogi, "Design of Composite Driveshafts for Automotive Applications," SAE International, Warrendale, PA, SAE Technical Paper 2004-01–0485, Mar. 2004. doi: 10.4271/2004-01-0485.
[17] M. M. Shokrieh, A. Hasani, and L. B. Lessard, "Shear buckling of a composite drive shaft under torsion," *Compos. Struct.*, vol. 64, no. 1, pp. 63–69, Apr. 2004, doi: 10.1016/S0263-8223(03)00214-9.
[18] S. Saha and S. Bal, "Influence of nanotube content on the mechanical and thermo-mechanical behaviour of –COOH functionalized MWNTs/epoxy composites," *Bull. Mater. Sci.*, vol. 40, no. 5, pp. 945–956, Sep. 2017, doi: 10.1007/s12034-017-1433-x.
[19] L. S. Schadler, S. C. Giannaris, and P. M. Ajayan, "Load transfer in carbon nanotube epoxy composites," *Appl. Phys. Lett.*, vol. 73, no. 26, pp. 3842–3844, Dec. 1998, doi: 10.1063/1.122911.
[20] A. Allaoui, S. Bai, H. M. Cheng, and J. B. Bai, "Mechanical and electrical properties of a MWNT/epoxy composite," *Compos. Sci. Technol.*, vol. 62, no. 15, pp. 1993–1998, Nov. 2002, doi: 10.1016/S0266-3538(02)00129-X.
[21] N.-H. Tai, M.-K. Yeh, and J.-H. Liu, "Enhancement of the mechanical properties of carbon nanotube/phenolic composites using a carbon nanotube network as the reinforcement," *Carbon*, vol. 42, no. 12–13, pp. 2774–2777, 2004, doi: 10.1016/j.carbon.2004.06.002.
[22] V. Jain, S. Jaiswal, K. Dasgupta, and D. Lahiri, "Influence of carbon nanotube on interfacial and mechanical behavior of carbon fiber reinforced epoxy laminated composites," *Polym. Compos.*, vol. 43, no. 9, pp. 6344–6354, 2022, doi: 10.1002/pc.26943.
[23] M. Hassanzadeh-Aghdam, R. Ansari, and A. Darvizeh, "A new micromechanics approach for predicting the elastic response of polymer nanocomposites reinforced with randomly oriented and distributed wavy carbon nanotubes," *J. Compos. Mater.*, vol. 51, no. 20, pp. 2899–2912, Aug. 2017, doi: 10.1177/0021998317712571.
[24] F. T. Fisher, R. D. Bradshaw, and L. C. Brinson, "Fiber waviness in nanotube-reinforced polymer composites—I: Modulus predictions using effective nanotube properties," *Compos. Sci. Technol.*, vol. 63, no. 11, pp. 1689–1703, Aug. 2003, doi: 10.1016/S0266-3538(03)00069-1.
[25] V. Anumandla and R. F. Gibson, "A comprehensive closed form micromechanics model for estimating the elastic modulus of nanotube-reinforced composites," *Compos. Part Appl. Sci. Manuf.*, vol. 37, no. 12, pp. 2178–2185, Dec. 2006, doi: 10.1016/j.compositesa.2005.09.016.
[26] E. T. Thostenson and T.-W. Chou, "On the elastic properties of carbon nanotube-based composites: modelling and characterization," *J. Phys. Appl. Phys.*, vol. 36, no. 5, p. 573, Feb. 2003, doi: 10.1088/0022-3727/36/5/323.
[27] G. D. Seidel and D. C. Lagoudas, "Micromechanical analysis of the effective elastic properties of carbon nanotube reinforced composites," *Mech. Mater.*, vol. 38, no. 8, pp. 884–907, Aug. 2006, doi: 10.1016/j.mechmat.2005.06.029.
[28] J. Pan, L. Bian, H. Zhao, and Y. Zhao, "A new micromechanics model and effective elastic modulus of nanotube reinforced composites," *Comput. Mater.*

Sci., vol. 113, pp. 21–26, Feb. 2016, doi: 10.1016/j.commatsci.2015.11.009.

[29] M. Omidi, H. Rokni D.T., A. S. Milani, R. J. Seethaler, and R. Arasteh, "Prediction of the mechanical characteristics of multi-walled carbon nanotube/epoxy composites using a new form of the rule of mixtures," *Carbon*, vol. 48, no. 11, pp. 3218–3228, Sep. 2010, doi: 10.1016/j.carbon.2010.05.007.

[30] S. K. Georgantzinos, P. Antoniou, S. Markolefas, and G. Giannopoulos, "Finite element predictions on vibrations of laminated composite plates incorporating the random orientation, agglomeration, and waviness of carbon nanotubes," *Acta Mech.*, vol. 233, no. 5, pp. 2031–2059, May 2022, doi: 10.1007/s00707-022-03179-6.

[31] M. K. Hassanzadeh-Aghdam and J. Jamali, "A new form of a Halpin–Tsai micromechanical model for characterizing the mechanical properties of carbon nanotube-reinforced polymer nanocomposites," *Bull. Mater. Sci.*, vol. 42, no. 3, p. 117, Apr. 2019, doi: 10.1007/s12034-019-1784-6.

[32] M.-K. Yeh, T.-H. Hsieh, and N.-H. Tai, "Fabrication and mechanical properties of multi-walled carbon nanotubes/epoxy nanocomposites," *Mater. Sci. Eng. A*, vol. 483–484, pp. 289–292, Jun. 2008, doi: 10.1016/j.msea.2006.09.138.

[33] S. Kanagaraj, F. R. Varanda, T. V. Zhil'tsova, M. S. A. Oliveira, and J. A. O. Simões, "Mechanical properties of high density polyethylene/carbon nanotube composites," *Compos. Sci. Technol.*, vol. 67, no. 15, pp. 3071–3077, Dec. 2007, doi: 10.1016/j.compscitech.2007.04.024.

[34] K. Duan *et al.*, "A critical role of CNT real volume fraction on nanocomposite modulus," *Carbon*, vol. 189, pp. 395–403, Apr. 2022, doi: 10.1016/j.carbon.2021.12.083.

[35] J. F. Wang, J. P. Yang, L. -h. Tam, and W. Zhang, "Effect of CNT volume fractions on nonlinear vibrations of PMMA/CNT composite plates: A multiscale simulation," *Thin-Walled Struct.*, vol. 170, p. 108513, Jan. 2022, doi: 10.1016/j.tws.2021.108513.

[36] M. Tarfaoui, K. Lafdi, and A. El Moumen, "Mechanical properties of carbon nanotubes based polymer composites," *Compos. Part B Eng.*, vol. 103, pp. 113–121, Oct. 2016, doi: 10.1016/j.compositesb.2016.08.016.

[37] A. K. Kaw, *Mechanics of Composite Materials*, Second Edition. U.S.: CRC Press, 2006.

[38] J. C. H. Affdl and J. L. Kardos, "The Halpin-Tsai equations: A review," *Polym. Eng. Sci.*, vol. 16, no. 5, pp. 344–352, 1976, doi: 10.1002/pen.760160512.

[39] D. L. Logan, *A first course in the finite element method*, Fifth Edition. USA: Cengage Learning, 2011.

[40] EnginSoft, "Ansys Composite PrepPost: A user-friendly approach to analyze composite material structures." Accessed: Jul. 21, 2023. [Online]. Available: https://www.enginsoft.com/solutions/ansys-composite-preppost.html

[41] P. D. Soden, M. J. Hinton, and A. S. Kaddour, "Chapter 2.1 - Lamina properties, lay-up configurations and loading conditions for a range of fibre reinforced composite laminates," in *Failure Criteria in Fibre-Reinforced-Polymer Composites*, M. J. Hinton, A. S. Kaddour, and P. D. Soden, Eds., Oxford: Elsevier, 2004, pp. 30–51. doi: 10.1016/B978-008044475-8/50003-2.

[42] S. Paunikar and S. Kumar, "Effect of CNT waviness on the effective mechanical properties of long and short CNT reinforced composites," *Comput. Mater. Sci.*, vol. 95, pp. 21–28, Dec. 2014, doi: 10.1016/j.commatsci.2014.06.034.

[43] F. Aghadavoudi, H. Golestanian, and Y. Tadi Beni, "Investigating the effects of CNT aspect ratio and agglomeration on elastic constants of crosslinked polymer nanocomposite using multiscale modeling," *Polym. Compos.*, vol. 39, no. 12, pp. 4513–4523, 2018, doi: 10.1002/pc.24557.

[44] M. Garg, S. Sharma, and R. Mehta, "Pristine and amino functionalized carbon nanotubes reinforced glass fiber epoxy composites," *Compos. Part Appl. Sci. Manuf.*, vol. 76, pp. 92–101, Sep. 2015, doi: 10.1016/j.compositesa.2015.05.012.

[45] M. A. Badie, E. Mahdi, and A. M. S. Hamouda, "An investigation into hybrid carbon/glass fiber reinforced epoxy composite automotive drive shaft," *Mater. Des.*, vol. 32, no. 3, pp. 1485–1500, Mar. 2011, doi: 10.1016/j.matdes.2010.08.042.